*Journal of the Korean Nuclear Society*
*Volume 31, Number 6, pp.529~540, December 1999*

# Evaluation of Photonuclear Data of Mo, Zn, S and Cl for Applications

**Young-Ouk LEE, Yinlu HAN, Jeong-Yeon LEE, and Jonghwa CHANG**

Korea Atomic Energy Research Institute
150 Dukjin-dong, Yusong-gu, Taejon 305-353, Korea
yolee@lui.kaeri.re.kr

(Received May 29, 1999)

## Abstract

As part of IAEA CRP on "Compilation and evaluation of photonuclear data for applications", we evaluated photoproduction data of Mo, Zn, S and Cl isotopes for medical use and biological applications. Available experimental data were collected and their discrepancies were analyzed to select or reconstruct the representative data set. The photoabsorption cross sections were then evaluated by applying the Giant Dipole Resonance (GDR) model for the energies below about 30 MeV and the quasi-deuteron model for energies below 140 MeV. The resulting representative photoabsorption data were given as input for the theoretical calculations for the emission process of light nuclei including neutron, proton, deuteron, triton, $^{3}$He, alpha particles and gamma rays by use of the Hauser-Feshbach and the preequilibrium model.

**Key Words** : photonuclear reaction data, giant dipole resonance, quasi-deuteron model, MeV range 0-140,molybdenum, zinc, sulphur, chlorine

## 1. Introduction

Evaluated photonuclear data are important for a variety of applications such as [1,2]

- radiation protection and dosimetry of photoneutron produced by electron or photon accelerators in medical applications,
- calculations of absorbed dose in a human body during radiotherapy,
- physics and technology of fission reactors and fusion reactors,
- activation analysis, safeguards and inspection technologies,
- nuclear waste transmutation, and astrophysics.

In response to the growing needs for photonuclear data, the IAEA initiated a Coordinated Research Project (CRP) under the title "Compilation and evaluation of photonuclear data for applications". As part of this project, we evaluated the photoproduction data of $^{99}$Mo which

is needed in $^{99}$Tc production for medical uses, and the photonuclear data of Mo, Zn, S and Cl isotopes for biological applications.

Chapter II deals with the evaluations and analysis of experimental data. Chapter III describes theoretical models and evaluation techniques applied in the work. In chapter IV, evaluated cross sections are presented and compared with experimental data. Finally, we summarize this work in Chapter V.

## 2. Analysis of Experimental Data

### 2.1. $^{92,94,96,98,100}$Mo

The natural Mo consists of seven isotopes, i. e. $^{92}$Mo (14.84 %), $^{94}$Mo (9.25 %), $^{95}$Mo (15.92 %), $^{96}$Mo (16.68 %), $^{97}$Mo (9.55 %), $^{98}$Mo (24.13 %) and $^{100}$Mo (9.63 %). The measured data of photoneutron cross sections for $^{92,94,96,98,100}$Mo were first performed in 1974 by H. Beil *et al.* [3] in the incident photon energy region from the threshold up to 30 MeV. The experimental data of the ($\gamma$, n+np), ($\gamma$, 2n+2np), ($\gamma$, 3n), ($\gamma$, xn) reactions and total neutron production were given respectively. The quasi-monoenergetic photon beams were used in measuring photoneutron data. There are no experimental data reported up to now for $^{95,97}$Mo.

### 2.2. $^{64,66,67,68,70}$Zn

The natural Zn consists of five isotopes, i. e. $^{64}$Zn (48.60 %), $^{66}$Zn (27.90 %), $^{67}$Zn (4.10 %), $^{68}$Zn (18.80 %) and $^{70}$Zn (0.60 %). The measured data of photoneutron cross sections in the incident photon energy region from the threshold to 24 MeV were first performed by Goryachev *et al.* [4] for $^{66,67,68,70}$Zn in 1982. As for $^{64}$Zn, most of the work of measuring photoneutron cross sections were carried out from 1951 to 1982. The experimental data of Katz *et al.* [5], Carlos *et al.* [6] and Goryachev *et al.* basically agree according to the shapes, but there are differences in the magnitudes. The measured data of Bianco *et al.* [7,8] and Coote *et al.* [9] are in agreement with Goryachev' s data. Most of the measuring work used the same method, in which the photoneutron cross sections for reactions ($\gamma$, n) + ($\gamma$, np) and ($\gamma$, 2n) were measured with monochromatic photon beams in the energy range of 8~30 MeV and a high efficiency neutron detecting system. Photoneutron yield curves were obtained for the isotopes $^{64,66,67,68,70}$Zn, then the cross sections were calculated from the yields by means of the Penfold-Leiss method [4] with the step of 1.0 MeV in the Goryachev' s work.

The magnitude of Katz' s data is quite different from others and there is no information on error analyses. In our evaluation, Katz' s data were excluded and Goryachev' s and Bianco' s experimental data were used to guide the theoretical calculations.

### 2.3. $^{32,34}$S

The natural S consists of four isotopes, i. e., $^{32}$S (95.02 %), $^{33}$S (0.75 %), $^{34}$S (4.21 %) and $^{36}$S (0.02 %). The experimental data are from Veyssiere *et al.* [10] and Katz *et al.* [5]. Veyssiere *et al.* gave the cross sections of the ($\gamma$, n + np), ($\gamma$, np), ($\gamma$ , 2n) reactions and photoneutron productions, and performed an analysis of the competition among the ($\gamma$,n), ($\gamma$, np) and ($\gamma$, 2n) exit channels. Katz *et al.* gave only $^{32}$S($\gamma$, np)$^{30}$P reaction cross sections. The cross sections for the $\gamma$ + $^{34}$S reaction were measured by Y. I. Assafiri *et al.* [11] in 1984 and 1986, giving the photoabsorption cross section and ($\gamma$, n), ($\gamma$,p), ($\gamma$, 2n) and ($\gamma$, np) reaction cross sections from the threshold to 26 MeV.

The experimental data of Veyssiere *et al.* and

Assafiri *et al.* were used to guide the theoretical calculations.

### 2.4. $^{35,37}$Cl

The natural Cl consists of two isotopes, i. e. $^{35}$Cl (75.77%) and $^{37}$Cl(24.23 % ). The measurements of photoneutron cross sections for $^{nat}$Cl were first performed by A. Veyssiere *et al.* [10] for the incident photon energy region from the threshold to 28 MeV in 1974. The experimental data of the ($\gamma$, n+np) and ($\gamma$, 2n+2np) reactions and total neutron production cross sections were given. The competition between the ($\gamma$, n), ($\gamma$, np), and ($\gamma$, 2n) exit channels was analysed.

## 3. Theoretical Models and Evaluation Techniques

There is no nuclear force and charge interaction between the photon and the nucleus, and thus the photonuclear reaction is induced by electromagnetic interaction. At low energies, below about 30 MeV, the Giant-Dipole Resonance (GDR) is the dominant excitation mechanism, where a collective bulk oscillation of the neutrons against the protons occurs. At higher energies below 140 MeV, the threshold for the pion production, where the wavelength of the photon decreases, the photoabsorption on a neutron-proton (quasi-deuteron: QD) which has a large dipole moment becomes important. Therefore, the photoabsorption cross section can be expressed as the sum of $\sigma_{GDR}(\varepsilon_\gamma)$ and $\sigma_{QDM}(\varepsilon_\gamma)$,

$$\sigma_{abs}(\varepsilon_\gamma) = \sigma_{GDR}(\varepsilon_\gamma) + \sigma_{QDM}(\varepsilon_\gamma). \quad (1)$$

In this work, photoabsorption cross sections in the GDR region were evaluated with GUNF code [12], in which $E_1$ and $E_2$ radiations are considered. The formulas of strength functions for $E_1$ and $E_2$ radiations used in the code are:

i ) Lorentzian form with Energy-dependent Damping Width for E1 Radiation [13] :

$$f_{E_1}(\varepsilon_\gamma) = \sum_{i=1}^{n} \frac{\sigma_i \varepsilon_\gamma \Gamma_i \Gamma_i(\varepsilon_\gamma)}{(\varepsilon_\gamma^2 - E_i^2)^2 + \varepsilon_\gamma^2 \Gamma_i^2(\varepsilon_\gamma)} \quad (2)$$

with

$$\Gamma_i(\varepsilon_\gamma) = \Gamma_i \frac{\varepsilon_\gamma^2 + 4\pi^2 T^2}{E_i^2} \quad (3)$$

where $\sigma_i$, $E_i$, and $\Gamma_i$ denote the peak cross section, peak energy, and width at half-maximum of the $i$-th peak, and

$$T^2 = \frac{B_n - \Delta - \varepsilon_\gamma}{a} \quad (4)$$

where $B_n$, $\Delta$, and $a$ denote the neutron binding energy, paring correction energy, and level density parameter.

ii ) Lorentzian Strength Function for $E_2$ Radiation:

$$f_{E_2}(\varepsilon_\gamma) = \frac{\sigma \varepsilon_\gamma^{-1} \Gamma^2}{(\varepsilon_\gamma^2 - E^2)^2 + \varepsilon_\gamma^2 \Gamma^2} \quad (5)$$

where $\sigma$, $E$, and $\Gamma$ denote the peak cross section, peak energy, and width at half-maximum of $E_2$ radiation.

The photonuclear absorption cross section is the sum of all the partial cross sections:

$$\sigma_{abs} = \sigma_{\gamma,n} + \sigma_{\gamma,p} + \sigma_{\gamma,d} + \sigma_{\gamma,t} + \sigma_{\gamma,He^3} + \sigma_{\gamma,\alpha} + \sigma_{\gamma,2n} + \ldots, \quad (6)$$

and photoneutron cross section is the sum of neutron producing cross sections as

$$\sigma_{\gamma,xn} = \sigma_{\gamma,n} + \sigma_{\gamma,np} + \sigma_{\gamma,2n} + \sigma_{\gamma,2np} + \sigma_{\gamma,3n} + \ldots \quad (7)$$

In the case of existence of the measured

photoabsorption cross sections, the resonance parameters can be adjusted by fitting the available experimental data of photoabsorption cross sections. When there is no measured photoabsorption cross section, the photoneutron cross sections can be used to approximate the photoabsorption cross sections for heavy nuclei, since contributions from photoproton reactions and other reactions producing complex charged particles are suppressed by the Coulomb barrier. However, in light nuclei where the photoproton cross section is no longer small, the resonance parameters are adjusted in such a way that the decaying model calculation with the initial nuclear excitation reproduces available photonuclear reaction measurements. The GUNF code uses Hauser-Feshbach and exciton models for decaying model calculations to adjust the resonance parameters when only photoneutron measurements are given.

The QDM photoabsorption cross section $\sigma_{QDM}(\varepsilon_\gamma)$ is expressed in terms of the quasi-deuteron model which uses a Levinger-type theory to relate the nuclear photoabsorption cross section to the experimental deuteron photodisintegration cross section $\sigma_d(\varepsilon_\gamma)$,

$$\sigma_{QDM}(\varepsilon_\gamma) = L\frac{NZ}{A}\sigma_d(\varepsilon_\gamma)f(\varepsilon_\gamma) \qquad (8)$$

where the Levinger parameter was derived to be $L$=6.5, and $f(\varepsilon_\gamma)$ is the Pauli-blocking function, which reduces the free deuteron cross section $\sigma_d(\varepsilon_\gamma)$ to account for Pauli-blocking of the excited neutron and proton by the nuclear medium. NZ is the total number of neutron-proton pairs inside the nucleus, and the free deuteron cross section is as follows:

$$\sigma_d(\varepsilon_\gamma) = 61.2\frac{(\varepsilon_\gamma - 2.224)^{\frac{3}{2}}}{\varepsilon_\gamma}\text{mb}. \qquad (9)$$

The Pauli-blocking function was derived in the Ref. [14] to be a multidimensional integral whose solution could be well approximated in the energy range 20 to 140 MeV by a polynomial, as follows:

$$\begin{aligned} f(\varepsilon_\gamma) \;=\; & 8.3714\times10^{-2} - 9.8343\times10^{-3}\varepsilon_\gamma \\ & + 4.1222\times10^{-4}\varepsilon_\gamma^2 \\ & -3.4762\times10^{-6}\varepsilon_\gamma^3 + 9.3537\times10^{-9}\varepsilon_\gamma^4 \end{aligned} \qquad (10)$$

Since the Pauli-blocking function needs to be defined at all energies, the exponential shape was used for energies below 20 MeV and above 140 MeV, as follows:

$$f(\varepsilon_\gamma) = e^{-\frac{D}{\varepsilon}} \qquad (11)$$

where D is a constant, 73.3 MeV for energy $\varepsilon_\gamma <$ 20 MeV and 24.2 MeV for energy $\varepsilon_\gamma >$ 140 MeV, respectively.

When the photoabsorption cross sections were established, the decaying processes including n, p, d, t and $\alpha$ particle emission up to 140 MeV were calculated using GNASH code [15]. The spherical optical model was used to calculate the transmission coefficients. The Hauser-Feshbach theory with full angular momentum and parity conservation calculated the equilibrium emission [16]. The preequilibrium theory was used to describe the processes of preequlibrium emission, and damping to equilibrium, during the evolution of the reaction. The theory for calculating photonuclear angular distributions, enabling a determination of the double differential cross sections of ejectiles and the multiple-preequilibrium emission processes which become important when the photon energy exceeds about 50 MeV were included in the calculation. The file of discrete level information and ground-state masses, spin and parities were provided, the mass values were based upon an interim set from Wapstra obtained prior to the 1988 publication, and supplemented in the case of unmeasured

masses with values from the Moller and Nix calculations. The optical potential parameters were taken from Ref [17].

## 4. Calculated Results

### 4.1. Resonance Parameters

Spherical nuclei are found around closed shells where all the single-particle states are fully occupied. On the other hand, many single-particle states are available for nuclei between closed shells. In general, the GDR has for spherical nuclei a single peak and for deformed nuclei double peak shapes, with a gross or fine structures in both cases.

In the present work, we employed a Lorentzian strength function of single peak form for Mo isotopes which are close to a major shell closure. For Zn, S, and Cl isotopes which are located between closed shells, we employed a Lorentzian strength function of double peak form.

The resonance parameters for $\gamma$ + $^{92,94,96,98,100}$Mo were obtained based on the experimental data of photoneutron cross sections approximated as photoabsorption cross sections.

For $^{64,66,67,68,70}$Zn, the photoneutron cross sections can not be used to approximate the photoabsorption cross sections since the photoproton and the photoalpha cross sections are no longer small. The resonance parameters were adjusted to better reproduce the experimental data of photoneutron cross sections.

The resonance parameters for the $\gamma$ + $^{32,34}$S reaction were obtained based on the experimental data of photoneutron cross sections with the same method as for the case of Zn isotopes. For the $\gamma$ + $^{33,36}$S reaction, the parameters of the $^{34}$S were used, since there are no experimental data.

The resonance parameters for the $\gamma$ + $^{35,37}$Cl reaction were obtained based on the experimental data of photoneutron cross sections for the $\gamma$ + $^{nat}$Cl reaction with the same method as for the case of Zn and S isotopes.

**Table 1. The Giant Resonance Parameters. The Units of $\sigma_i$, $\gamma_i$ and $E_i$ are mb, MeV and MeV, Respectively**

| | $\sigma_1^{E_1}$ | $\Gamma_1^{E_1}$ | $E_1^{E_1}$ | $\sigma^{E_2}$ | $\Gamma^{E_2}$ | $E^{E_2}$ |
|---|---|---|---|---|---|---|
| $^{92}$Mo | 162 | 5.95 | 17.11 | 976 | 2.65 | 15.58 |
| $^{94}$Mo | 168 | 6.05 | 16.75 | 258 | 2.75 | 13.45 |
| $^{96}$Mo | 156 | 8.04 | 16.43 | 129 | 3.90 | 17.38 |
| $^{98}$Mo | 110 | 12.39 | 16.37 | 410 | 3.45 | 16.13 |
| $^{100}$Mo | 122 | 10.03 | 15.72 | 294 | 4.07 | 16.86 |
| | $\sigma_1^{E_1}$ | $\Gamma_1^{E_1}$ | $E_1^{E_1}$ | $\sigma_2^{E_1}$ | $\Gamma_2^{E_1}$ | $E_2^{E_1}$ |
| $^{64}$Zn | 38 | 5.95 | 16.32 | 48 | 7.89 | 18.28 |
| $^{66}$Zn | 59 | 5.94 | 16.21 | 25 | 7.73 | 18.46 |
| $^{67}$Zn | 75 | 9.62 | 17,22 | 72 | 5.85 | 20.96 |
| $^{68}$Zn | 65 | 6.79 | 16.15 | 37 | 5.42 | 19.36 |
| $^{70}$Zn | 54 | 9.96 | 16.71 | 14 | 6.22 | 19.83 |
| | $\sigma_1^{E_1}$ | $\Gamma_1^{E_1}$ | $E_1^{E_1}$ | $\sigma_2^{E_1}$ | $\Gamma_2^{E_1}$ | $E_2^{E_1}$ |
| $^{32}$S | 37 | 8.60 | 20.19 | 3 | 10.32 | 27.27 |
| $^{34}$S | 28 | 6.10 | 17.30 | 42 | 4.63 | 22.05 |
| | $\sigma_1^{E_1}$ | $\Gamma_1^{E_1}$ | $E_1^{E_1}$ | $\sigma_2^{E_1}$ | $\Gamma_2^{E_1}$ | $E_2^{E_1}$ |
| $^{35}$Cl | 41 | 8.97 | 18.28 | 16 | 8.20 | 21.15 |
| $^{37}$Cl | 18 | 11.92 | 19.89 | 24 | 9.73 | 23.90 |

The resulting parameters for Mo, Zn, S and Cl isotopes are listed in Table 1.

### 4.2. Photonuclear Cross Sections

In Fig. 1, the calculated results for the $\gamma$ + $^{100}$Mo reaction cross sections are compared with the experimental data of Beil *et al.* [3]. It is shown that the overall shape and magnitude of photoneutron cross sections are in good agreement with the experimental data. $^{99}$Mo, the medical radioisotope of interest, can be induced from the $^{100}$Mo($\gamma$, n)$^{99}$Mo reaction. The production cross sections for $^{99}$Mo are also given in Fig. 1. The calculated results show that the production cross sections of

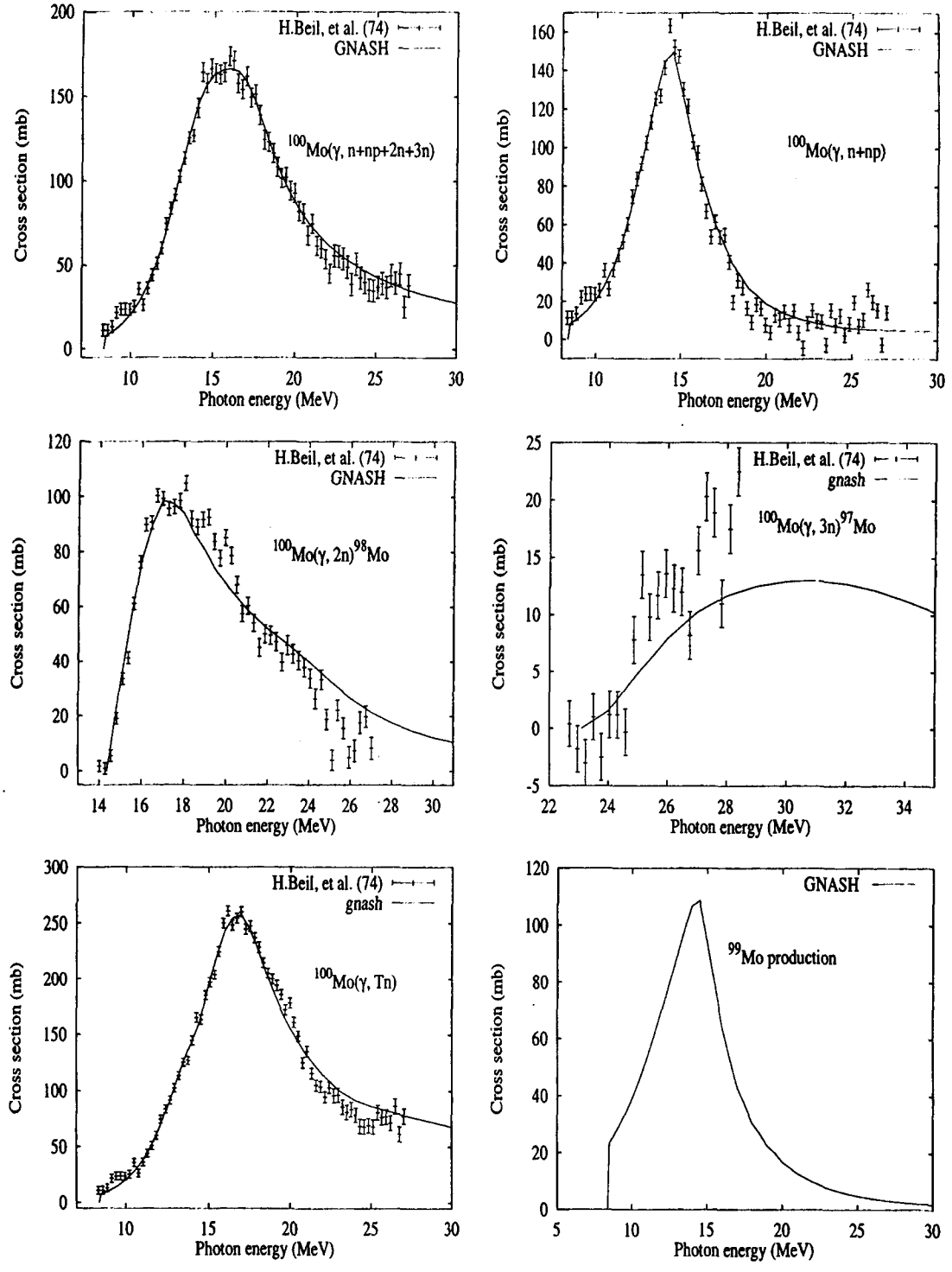


**Fig. 1. The Comparison of Calculated Results with Experimental Data for $^{100}$Mo Photonuclear Reaction Cross Sections**

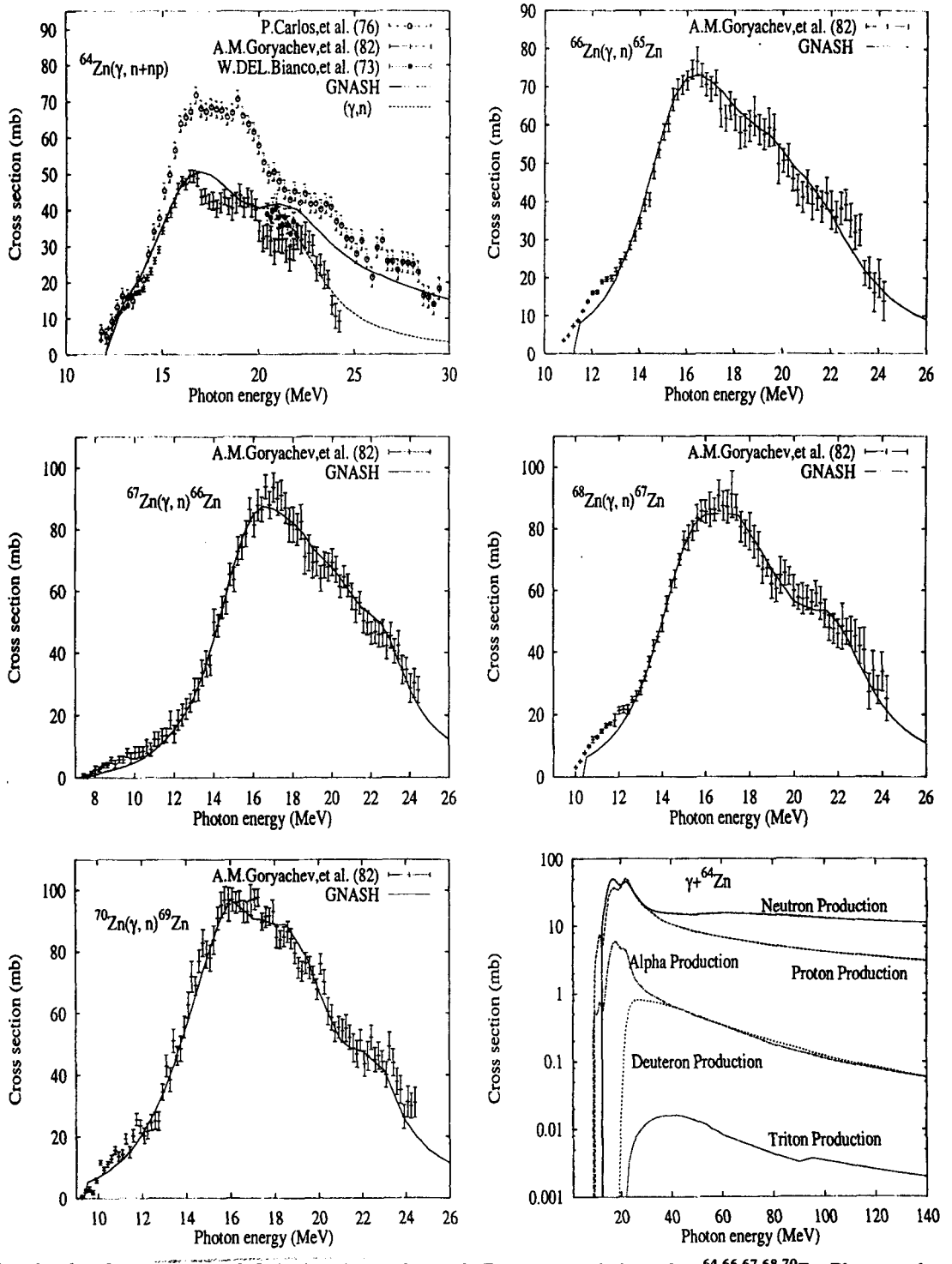


**Fig. 2. The Comparison of Calculated Results with Experimental Data for $^{64,66,67,68,70}$Zn Photonuclear Reaction Cross Sections**

$^{99}$Mo increase sharply from incident photon energies of 8 MeV up to around 15 MeV, and decrease rapidly above 15 MeV.

The calculated results for $^{64,66,67,68,70}$Zn($\gamma$, n) reaction cross sections are compared with the experimental data in Fig. 2. The calculation photoneutron cross section agree well with the experimental data of Goryachev et al. [4] and Bianco et al. [8]. For the $^{64}$Zn($\gamma$, n+np) reaction, the calculated results are lower than the experimental data of Carlos et al. [6] for incident photon energies $E_\gamma > 15$ MeV, since the experimental data of Goryachev et al. [4] were used to guide theoretical calculation. The photoneutron, photoproton, photoalpha cross sections and the particle production cross section are also given in Fig. 2 for the $^{64}$Zn isotope. The results show that the photoproton and the photoalpha cross sections are no longer small, and around 22 MeV the photoproton cross section exceeds the photoneutron cross section for the $\gamma$ + $^{64}$Zn reaction.

The comparison of calculated results with the experimental data for $\gamma$ + $^{32}$S reaction cross sections is given in Fig. 3. The calculated photoneutron cross sections and total neutron production cross sections agree with experimental data for the $\gamma$ + $^{32}$S reaction, and the calculated results of the $^{32}$S($\gamma$, 2n) reaction agree with the existing experimental data. For the $^{32}$S($\gamma$, np)$^{30}$P reaction, the theoretical results are in agreement with the experimental data of Veyssiere et al. [10] for incident photon energies $E_\gamma < 26$ MeV. For energies $E_\gamma \geq 26$ MeV, the calculated results are higher than the experimental data of Veyssiere, but are lower than those of Katz et al. [5]. The n, p, d, t and $\alpha$ emission cross sections as well as the production cross section for the $\gamma$ + $^{32}$S reaction were calculated up to 140 MeV, and are shown in Fig. 3.

The calculated results for $\gamma$ + $^{35,37}$Cl reaction cross sections are compared with the experimental data [10] in Fig. 4. Since the experimental data are for natural nucleus, the calculated results for $^{35}$Cl and $^{37}$Cl were transformed into those for a natural nucleus with the relation:

$$\sigma(^{nat}\mathrm{Cl}) = \sigma(^{35}\mathrm{Cl}) * 0.7577 + \sigma(^{37}\mathrm{Cl}) * 0.2423. \quad (12)$$

The calculated results are basically in agreement with experimental data for the ($\gamma$, n + np), ($\gamma$, 2n+2np) and ($\gamma$,n+np+2(2n+2np)) reactions. The calculated results for the photoabsorption, the particle emission and the particle production cross sections for energies up to 140 MeV are also given in Fig. 4.

## 5. Conclusions

Available experimental data were collected and their discrepancies were analyzed to select or reconstruct the representative data set. The photoabsorption cross sections were then evaluated by applying the Giant Dipole Resonance (GDR) model for the energies below about 30 MeV, and the quasi-deuteron model for energies below 140 MeV, which is the threshold for the pion production. The resulting representative photoabsorption data were given as input for the theoretical calculations for the emission process of light nuclei, including neutron, proton, deuteron, triton, $^3$He, alpha particles and gamma rays by the use of the Hauser-Feshbach and the preequilibrium model. Appropriate optical model parameters were applied to prepare the transmission coefficients for the Hauser-Feshbach statistical model. The theoretical results are in good agreement with existing experimental data for incident photon energies below 30 MeV. Therefore, our evaluations are reliable and are recommended for this energy region. Above the GDR region up to 140 MeV, where experimental

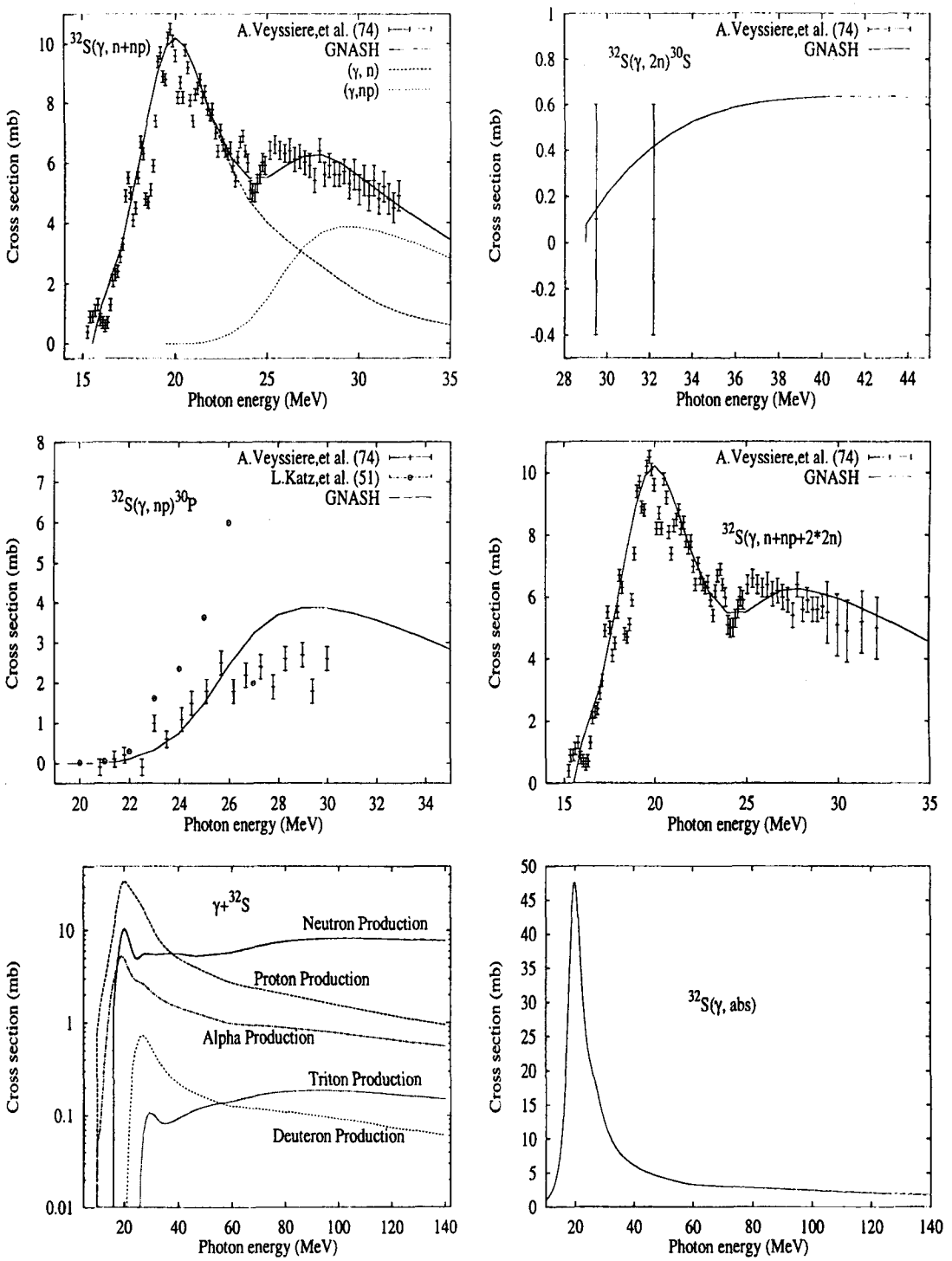


**Fig. 3. The Comparison of Calculated Results with Experimental Data for $^{32}$S Photonuclear Reaction Cross Sections**

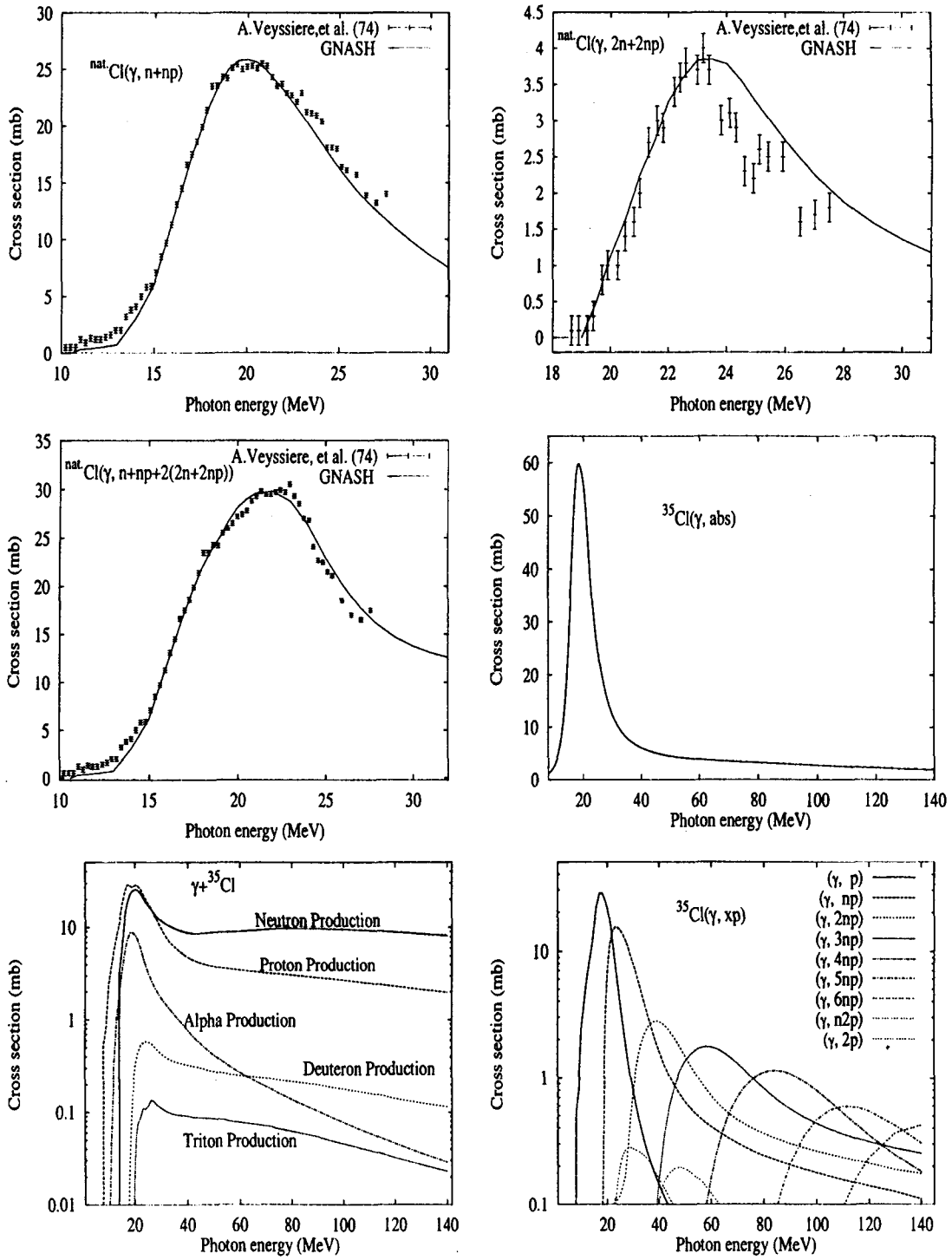


**Fig. 4. The Comparison of Calculated Results with Experimental Data for $^{35,37}$Cl Photonuclear Reaction Cross Sections**

data are scarce, the calculated results using quasi-deuteron, Hauser-Feschbach, and preequilibrium model need to be validated when new measurements become available.

## Acknowledgements

This work was performed under the auspices of the Korea Ministry of Science and Technology as one of the long-term nuclear R&D programs, and by IAEA Contract No.10547/R0. One of the authors (Y. HAN) is grateful to the Korea Science and Engineering Foundation for giving him an opportunity to carry out this work under the Brain Pool program.

## References

1. Y. O. Lee, T. Fukahori, and J. Chang, "Evaluation of Photoneutron Cross Sections for Ta-181 in Giant Resonance Region," *in Korean Physics Society Fall Conference, Oct.* 24-25, Kyonggi Univ., (1997).
2. Y. O. Lee, T. Fukahori, and J. Chang, "Evaluation of Photonuclear Reaction Data on Tantalum-181 up to 140 MeV." *J. of Nucl. Sci. and Tech.*, vol. 350, p. 685, (1998).
3. H. Beil, R. Bergere, P. Carlos, A. Lepretre, and A. Miniac, "A Study of the Photoneutron Contribution to the Giant Dipole Resonance in Doubly Even Mo Isotopes." *Nucl. Phys.*, vol. A219, pp. 61,427, (1974).
4. A. M. Goryachev, B. S. Ishkhanov, I. M. Kapitonov, I. M. Piskarev, V. G. Shevchenko, and O. P. Shevchenko, "The Studying of the Photoneutron Reactions Cross Sections in the Region of the Giant Dipole Resonanse in Zinc, Germanium, Selenium, and Strontium Isotopes." *Voprosy Teoreticheskoj adernoj Fiziki*, vol. 8, p. 121, (1982).
5. L. Katz and A. G. W. Cameron, "The Solution of X-Ray Activation Curves for Photonuclear Cross Sections." *J. Canada Phys.*, vol. 29, p. 518, (1951).
6. P. Carlos, H. Beil, R. Bergere, J. Fagot, A. Lepretre, A. Veyssiere, and G. V. solodukhov, "A study of the Photoneutron Contribution to the Giant Dipole Resonance of Nuclei in the A=64-86 Mass Region." *Nucl. Phys.*, vol. A258, p. 365, (1976).
7. W. Bianco and W. E. Stephens, "Photonuclear Activation by 20.5 MeV Gamma Rays." *Phys. Rev.*, vol. 126, p. 709, (1962).
8. W. Bianco *et al.*, "$^{64}$Zn($\gamma$,n)$^{63}$Zn Cross Section from 20.4 to 21.9 MeV." *J. Canada Phys.*, vol. 51, p. 1302, (1973).
9. G. Coote *et al.*, "Cross Sections for the ($\gamma$,n) Reaction in $^{63}$Cu, $^{65}$Cu, $^{64}$Zn, $^{121}$Sb, and $^{141}$Pr, Measured with Monochromatic gamma rays." *Nucl. Phys.*, vol. 23, p. 468, (1961).
10. A. Veyssiere *et al.*, " A Study of the Photoneutron Contribution to the Giant Dipole Resonance of s-d Shell Nuclei." *Nucl. Phys.*, vol. A227, p. 513, (1974).
11. Y. I. Assafiri *et al.*, "Photoneutron Cross Section of $^{34}$S," *Nucl. Phys.*, vol. A413, p. 416, (1984).
12. J. Zhang, "Illustration of Photonuclear Data Calc. with GUNF Code." *Commu. of Nucl. Data Prog.*, vol. 19, p. 33, (1998).
13. J. Kopecky and M. Uhl, "Test of Gamma-Ray Strength Functions in Nuclear-Reaction Model-Calculations." *Phys. Rev.* C, vol. 41, pp. 1941--1955, (1990).
14. M. Chadwick et al, "Pauli-blocking in the Quasideuteron Model of Photoabsorption." *Phys. Rev.* C, vol. 44, p. 814, (1991).
15. M. Chadwick et al, "Photonuclear Reactions in the GNASH code." Tech. Rep. UCRL-ID-118721, Lawrence Livermore National

Laboratory, Livermore, CA, (1994).
16. M. B Chadwick, P. . Young, and S. Chiba, " Photonuclear angular distribution systemics in the quasideuteron regime." *Journal of Nuclear Science and tehnology*, vol. 32, p. 1154, (1995).
17. C. M. Perey and F. G. Perey, "Compilation of Phenomenological Optical Model Parameters." *Atomic Data and Nucl. Data Tables*, vol. 17, pp. 1-101, (1976).